



Modulation of matrix mineralization by Vwc2-like protein and its novel splicing isoforms

Yoshio Ohyama^a, Michitsuna Katafuchi^b, Ahmed Almekhadi^a, Sundharamani Venkitapathi^a, Haytham Jaha^a, Jason Ehrenman^a, Joseph Morcos^a, Reem Aljamaan^a, Yoshiyuki Mochida^{a,*}

^a Department of Periodontology and Oral Biology, Boston University, Henry M. Goldman School of Dental Medicine, 700 Albany Street, Boston, MA 02118, USA

^b Department of Oral Rehabilitation, Section of Fixed Prosthodontics, Fukuoka Dental College, 2-15-1 Tamura Sawara-Ku, Fukuoka 814-0193, Japan

ARTICLE INFO

Article history:

Received 9 December 2011

Available online 22 December 2011

Keywords:

Cysteine knot protein (CKP)
von Willebrand factor C domain-containing protein 2-like (Vwc2l)
Splicing isoforms
Matrix mineralization
Osterix

ABSTRACT

In search of new cysteine knot protein (CKP) family members, we found a novel gene called von Willebrand factor C domain-containing protein 2-like (Vwc2l, also known as Brorin-like) and its transcript variants (Vwc2l-1, Vwc2l-2 and Vwc2l-3). Based on the deduced amino acid sequence, Vwc2l-1 has a signal peptide and 2 cysteine-rich (CR) domains, while Vwc2l-2 lacks a part of 2nd CR domain and Vwc2l-3 both CR domains. Although it has been reported that the expression of Brorin-like was predominantly observed in brain, we found that Vwc2l transcript variants were detected in more ubiquitous tissues. In osteoblasts, the induction of Vwc2l expression was observed at matrix mineralization stage. When Vwc2l was stably transfected into osteoblasts, the matrix mineralization was markedly accelerated in Vwc2l-expressing clones compared to that in the control, indicating the modulatory effect of Vwc2l protein on osteoblastic cell function. The mechanistic insight of Vwc2l-modulation was further investigated and we found that the expression of Osterix, one of the key osteogenic markers, was significantly increased by addition of all Vwc2l isoform proteins. Taken together, Vwc2l is a novel secreted protein that promotes matrix mineralization by modulating Osterix expression likely through TGF- β superfamily growth factor signaling pathway. Our data may provide mechanistic insights into the biological functions of this novel CKP member in bone and further suggest a novel approach to enhance osteoblast function, which enables to accelerate bone formation, regeneration and healing.

© 2011 Elsevier Inc. All rights reserved.

1. Introduction

In 1965, Urist M.R published the results of experiment that was to mark a turning point in experimental bone bioengineering, demonstrating the ability of decalcified bone matrix (DBM) to induce ectopic bone/cartilage formation. The morphogens in DBM that induce such skeletogenesis were named as bone morphogenetic proteins (BMPs) [1]. Since then, more than 20 members of BMPs have been identified and belong to Transforming Growth Factor (TGF)- β superfamily [2]. It is now well accepted that BMPs are potent effectors in almost all crucial biological events, e.g. development, maintenance and regeneration of organs/tissues, e.g. bone, cartilage, periodontium, kidney, heart, etc. [3–8]. Recombinant human BMP-2 is now US Food and Drug Administration (FDA) approved and has been applied to various clinical settings including craniofacial reconstruction, and bone/cartilage repair and regeneration [9–13]. However, there are still several problems for the clinical use of BMPs; poor expression control of BMP genes when administered by vector

transfer systems, poor control of retention and release of BMPs upon its transplantation, inefficient control of broad biological functions of BMPs, etc. [14,15]. Thus, a clear understanding as to how BMP functions are controlled *in vivo* is crucial for the development of efficient BMP-based treatments. It has become clear that the functions of BMPs are controlled at several levels, i.e. extracellular, cell surface and intracellular levels [16–20]. There are a number of extracellular modulators identified as BMP antagonists, such as chordin and noggin, which exert inhibitory effects on BMP functions [21–24]. However, at present, little is known about the extracellular modulators that promote BMP functions. Such positive growth factor regulators could be useful to develop a more efficient local transfer system.

Very recently, in an effort to identify BMP-binding proteins, we have established a bioinformatics approach [25,26] with some modifications, and identified a new gene which possesses a similar motif to known BMP antagonists. In this current study, we report the identification of novel Vwc2l transcript variants, the tissue distribution/gene expression pattern of these variants, and the effect of Vwc2l protein on osteoblast mineralization *in vitro* and on the expression of osteogenic markers induced by these isoform proteins.

* Corresponding author. Fax: +1 617 638 4942.

E-mail address: mochida@bu.edu (Y. Mochida).

2. Materials and methods

2.1. Cell culture

Human embryonic kidney 293 cells (Clontech) and mouse calvaria-derived MC3T3-E1 cells (subclone 4, ATCC; CRL-2593) were maintained in the same manner as previously reported [26].

2.2. Molecular cloning of mouse *Vwc2l* cDNA

The cDNAs containing the full length sequences of *Vwc2l* were isolated by reverse transcription-polymerase chain reaction (RT-PCR) using mouse brain-derived cDNA as a template. The sequences of the primers were as follows: forward primer, 5'-GCATCCCATG-GAAGGAGCTGAGTGTG-3' and reverse primer, 5'-CAACCCAGAAAGGTTTGCTGGTGACC-3'. The PCR conditions were as follows: 15 min at 95 °C; 30 s at 95 °C, 1 min at 60 °C, 1.5 min at 72 °C for 30 cycles. The PCR products were then ligated into the pcDNA3.1-V5/His-TOPO mammalian expression vector (Invitrogen) and the plasmids obtained were sequenced. During the course of molecular cloning of *Vwc2l*, we have obtained 2 transcript variants in addition to the longest transcript which is identical to the NCBI reference sequence (NM_177164). Thus, these variants were cloned and further characterized. The plasmids containing the coding sequence of either *Vwc2l*-1, -2 or -3 were generated by RT-PCR and successfully obtained (pcDNA3.1-Vwc2l-1-V5/His, pcDNA3.1-Vwc2l-2-V5/His, and pcDNA3.1-Vwc2l-3-V5/His, respectively).

2.3. Expression of *Vwc2l* isoforms

To investigate the *Vwc2l* gene expression in various tissues, Reverse-Transcription (RT)-PCR analysis was performed using cDNAs derived from mouse tissues including heart, brain, lung, kidney, calvaria and femur (C57BL/6 strain, 5 weeks, male) and MC3T3-E1 (MC) mouse osteoblastic cells. MC cells were maintained and plated onto 35 mm dishes at a density of 2×10^5 cells/dish. After reaching confluence, the medium was replaced with the one supplemented with 50 µg/ml of ascorbic acid and 1 mM of β-glycerophosphate (mineralization medium) (this time point will be referred to as day 0), and maintained for up to 35 days (fully mineralized stage). Cells were washed with phosphate buffered saline (PBS), and total RNA was extracted with TRIzol reagent solution (Invitrogen) at the end of every week. Mouse tissue samples were collected, and total RNA was extracted in the same manner. Two µg of the total RNA extract was used for RT using the Omniscript RT Kit (Qiagen). RT-PCR was performed using *Vwc2l* specific primers (forward primer: 5'-GGGATGGCTCTTCATATTCATGAAGC-3', reverse primer: 5'-CACAGTCTGCTTGCCTTGGCATTCGC-3') in the same manner as described above. Real time PCR analysis was performed in triplicate using the specific primers-probe for *Vwc2l*-1 (Applied Biosystems, ABI assay number: Mm01260094_m1) or glyceraldehyde-3-phosphate dehydrogenase (GAPDH, ABI assay number: 4308313). The mean fold changes in the expression of *Vwc2l* relative to that of GAPDH were calculated using the values obtained from MC cells at day 7 cDNA as a calibrator by means of $2^{-\Delta\Delta C_t}$ method as described previously [25,26]. Three independent experiments were performed and results were essentially identical.

2.4. Generation of MC cell-derived clones expressing higher levels of *Vwc2l*-1 protein and *in vitro* mineralization assay

MC cells were transfected with the pcDNA3.1-Vwc2l-1-V5/His vector or an empty pcDNA3.1-V5/His A vector (EV), and stably transfected cell clones were generated in the same manner as previously described [27]. The clones expressing various higher levels

of *Vwc2l*-1 proteins established above were selected and further subjected to an *in vitro* mineralization assay [27–29]. The control EV clone and *Vwc2l* clones were maintained and plated onto 35 mm culture dishes at a density of 2×10^5 cells/well. The medium was then changed to the mineralization medium in the same manner as described above and cultured for up to 28 days. The cell/matrix layers were washed with PBS, fixed with 100% methanol and stained with 1% Alizarin Red S (Sigma) to visualize the mineralized nodule formation at days 14 and 28. In order to determine *Vwc2l* protein levels, cultured media from EV clone and *Vwc2l* clones (#1 and #2) were collected and immunoprecipitated (IP) with anti-V5 antibody (Invitrogen). The samples were subjected to Western Blotting (WB) analysis with anti-V5 antibody in the same manner as previously reported [25,26].

2.5. Purification of *Vwc2l*-V5/His protein and the effect of purified *Vwc2l* proteins on osteogenic marker gene expression

In order to characterize the *Vwc2l* protein function, recombinant *Vwc2l* isoform proteins were generated and purified in the same manner as previously described [26]. Briefly, the 293 cells were transfected with the pcDNA3.1-Vwc2l-1-V5/His vector and cultured in the presence of 400 µg/ml of G418 (Gibco). The clones derived from G418-resistant cells were isolated, further grown under the same conditions, cultured media were collected, and subjected to IP-WB analysis with anti-V5 antibody. The clone which produced the highest level of *Vwc2l*-1-V5/His protein was further cultured and *Vwc2l*-1-V5/His protein from the cultured media was purified using a Ni-NTA agarose resin (Qiagen). Following the nickel column purification, the fraction was further purified by a Superdex-200 column (GE Healthcare) using a Hitachi D-7000 HPLC system. The purity of the *Vwc2l*-1-V5/His protein was assessed by Coomassie Brilliant Blue R-250 staining and WB analyses with anti-V5 antibody. The *Vwc2l*-2- and *Vwc2l*-3-V5/His proteins were also purified in the same manner as described. The purified *Vwc2l* isoform proteins were pooled, dialyzed against distilled water, lyophilized and dissolved in distilled water. The protein concentration was measured using a DC protein assay kit (Bio-Rad) and they were kept at –20 °C until use.

For osteogenic marker expression assay, MC cells were plated onto 35 mm dishes at a density of 2×10^5 cells/dish. On the following day, 500 ng/ml of the purified *Vwc2l* isoform proteins or bovine serum albumin (BSA) were added into cell culture and incubated for 24 h. The cDNA was synthesized derived from RNA collected from these cultures and used as templates. Real time PCR primers-probes of osteogenic markers used in this study were as follows; core binding factor 1/runx-related transcription factor 2 (Cbfa1/Runx2, Mm00501578_m1); osterix/sp7 (Osx, Mm00504574_m1); type I collagen alpha 2 chain (Col1a2, Mm00483888_m1); bone sialoprotein (Bsp, Mm00492555_m1); osteocalcin (Ocn, Mm01741771_g1). Real time PCR was performed and analyzed in the same manner as described above. The mean fold changes in the expression of each osteogenic marker relative to that of GAPDH were calculated using the values of cDNA derived from the cell culture treated with BSA as a calibrator.

3. Results and discussion

3.1. Novel transcript variants of *Vwc2l* gene

To identify a new member of the cysteine knot protein, we first obtained an amino acid sequence of mouse Ventroptin (GenBank accession no: AF247822) as a query sequence and performed a BLAST search in mouse genome (<http://www.ncbi.nlm.nih.gov/genome/seq/MmBlast.html>). The candidate sequences were then

obtained and a PSORT II program (<http://psort.nibb.ac.jp/form2.html>) was used to predict the cellular localization. This computational screen identified one possible extracellular molecule that has a signal peptide sequence. The predicted amino acid sequence of Vwc2l is 222 amino acid long, which has 2 characteristic cysteine-rich (CR) domains commonly found in CKP family (Fig. 1). This molecule has been reported as Brorin-like, which was first reported to be expressed predominantly in brain tissue [30]. The Vwc2l gene is localized at mouse chromosome 1 *in silico*, spans over 160 kb, and consisted of 4 exons (based on NCBI Gene ID: 320460). During the molecular cloning of Vwc2l gene, we identified that Vwc2l gene has three transcript variants, i.e. Vwc2l-1, Vwc2l-2 and Vwc2l-3. The Vwc2l-1 variant encodes the longest protein which was the same isoform as previously reported [30]. The Vwc2l-2 variant encodes 139 amino acid long isoform which lacks CR2 domain, while Vwc2l-3 102 amino acid long isoform lacking both CR domains (Fig. 1).

3.2. Expression of Vwc2l in skeletal tissues and its association with matrix mineralization

We next determined the expression levels of Vwc2l transcript variants in various mouse tissues. As shown in Fig. 2A (upper panel), the RT-PCR data demonstrated that the Vwc2l transcript variants were differentially expressed in the tissues examined, i.e. the expression level of Vwc2l-2 in femur/calvaria was higher than that of Vwc2l-1 and that of Vwc2l-3 was under detection level, the expression level of Vwc2l-3 in lung and heart was higher than that of other variants, and the expression levels of both Vwc2l-1 and Vwc2l-2 in kidney and brain were higher than that of Vwc2l-3. The relatively higher level of Vwc2l-1 expression in brain among tissues (Fig. 2A, upper band) was observed, consistent with the previous finding [30]. The expression level of GAPDH was comparable among these tissue samples (Fig. 2A, lower panel). Since exon 3 (based on NCBI Gene ID: 320460) is present only in Vwc2l-1 variant, the expression pattern of this specific transcript in MC cells during the course of cell differentiation and matrix mineralization was quantitatively investigated. Under the conditions of staining with Alizarin red, mineralized nodules were well formed at day 21 and further expanded at day 28 [31]. The expression level of Vwc2l-1 was markedly increased at day 28 and 35 (i.e. ~7-fold at day 28 and ~18-fold at day 35 compared to that of day 7, Fig. 2B), suggesting that Vwc2l-1 is potentially associated with matrix mineralization.

3.3. Vwc2l accelerates matrix mineralization in MC3T3-E1 osteoblastic cells

Since the expression of Vwc2l was detected in femur and calvaria (Fig. 2A) and increased at a time when mineralized nodules were fully formed (Fig. 2B), the effect of Vwc2l overexpression was investigated in MC3T3-E1 osteoblastic cells. As shown in Fig. 3A, the onset of mineralized nodule formation was clearly observed at day 28, but not at day 14 in the control EV clone while that was already evident at day 14 in both Vwc2l-overexpressing clones. The extent of mineralized nodule formation was greater in #1 and #2 clones than in the EV clone at any time points tested (Fig. 3A). To confirm the expression levels of Vwc2l overexpression in these clones, IP-WB analysis was performed using the cultured media derived from EV, #1 and #2 clones (Fig. 3B). The expression of Vwc2l-V5/His using anti-V5 antibody was successfully detected and the immunoreactivity derived from #2 cultured medium was greater than that of #1, demonstrating the expression level of Vwc2l was correlated with the timing and extent of accelerated mineralized nodule formation (Fig. 3A).

3.4. Effects of Vwc2l isoform proteins on osteoblast differentiation

To investigate the mechanistic insight of accelerated mineralized nodule formation in Vwc2l clones, we further examined the potential changes of osteoblast differentiation markers by the addition of Vwc2l isoform proteins in MC3T3-E1 cells. To confirm the levels of purified Vwc2l-V5/His isoform proteins produced by 293 cells, the same concentration of purified proteins together with BSA as a negative control were analyzed by WB analysis using anti-V5 antibody (Fig. 4A). The results showed that a smear band of Vwc2l-1-V5/His was observed at the molecular weight size of ~30 kDa area (Fig. 4A, lane 2), whereas rather sharp bands of Vwc2l-2-V5/His and Vwc2l-3-V5/His were detected at the molecular weight size of ~17 kDa and 14 kDa, respectively (Fig. 4A, lanes 3 and 4). The appearance of Vwc2l-1 isoform protein is different from that of other isoform proteins possibly due to potential post translational modification. This modification most likely occurs at the C-terminal part of Vwc2l-1 isoform lacking in both Vwc2l-2 and Vwc2l-3 isoforms (i.e. amino acid position 131–222). No immunoreactivity was observed when BSA was used (Fig. 4A, lane1). The equal amount of Vwc2l isoform proteins and BSA were then added into MC3T3-E1 cells and the expression levels of well-known osteogenic markers including Cbfa1, Osterix, type I collagen $\alpha 2$ chain,

Isoform 1:	1	MALHIHEACILLLVIPGLVTSAAISHEDYPADEGDQASSNDNLIFDDYRGKG	CVDDSGFV	60
Isoform 2:	1	MALHIHEACILLLVIPGLVTSAAISHEDYPADEGDQASSNDNLIFDDYRGKG	CVDDSGFV	60
Isoform 3:	1	MALHIHEACILLLVIPGLVTSAAISHEDYPADE-----		33

CR1				
Isoform 1:	61	YKLGERFFPGHSNCPVCALDGPVCDQPECPKIHPKCTKVEHNGCCPEC	KEVKNFCEYHG	120
Isoform 2:	61	YKLGERFFPGHSNCPVCALDGPVCDQPECPKIHPKCTKVEHNGCCPEC	KEVKNFCEYHG	120
Isoform 3:	34	-----DGPVCDQPECPKIHPKCTKVEHNGCCPEC	KEVKNFCEYHG	83

CR2				
Isoform 1:	121	KNYKILEEFKPSCEWCRCEPSNEVHCVAADCAVPECVNPITYEPOCCPVQ	KNGPNCFAG	180
Isoform 2:	121	KNYKILEEFKQV-----TALQELQ-----		139
Isoform 3:	84	KNYKILEEFKQV-----TALQELQ-----		102
***** . . :*::				
Isoform 1:	181	TTIIPAGIEVKGDCNICHCHNGDWWKPAQCSKRECQGKQTV		222
Isoform 2:		-----		
Isoform 3:		-----		

Fig. 1. The amino acid sequences of Vwc2l isoforms. Comparison of amino acid sequences of mouse Vwc2l isoform1, 2, and 3 is shown. The putative signal peptide sequence and cleavage site were predicted using the PSORT II program and are outlined with a light-blue box. Cysteine-rich (CR) region 1 and 2 are indicated by red boxes. Identical amino acids among isoforms are indicated by asterisk and the extent of similarity in amino acids among isoforms is by numbers of dots. Gaps are indicated by dashes. (For interpretation of the references to color in this figure legend, the reader is referred to the web version of this article.)

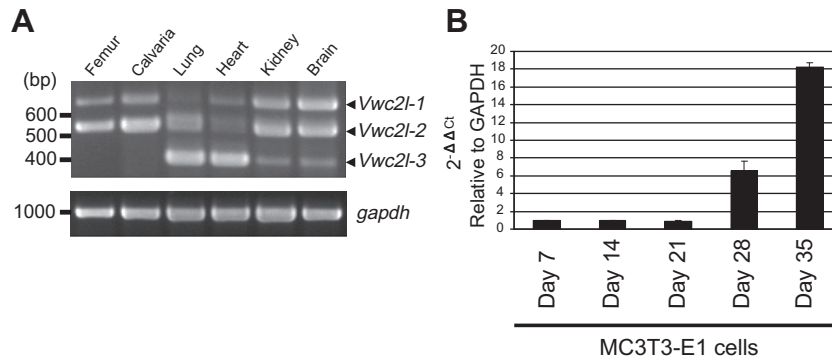


Fig. 2. Gene expression of Vwc2l isoforms. (A) RT-PCR analysis with Vwc2l-specific primers was performed. The expression of GAPDH was also examined and shown as a control. The size of the amplified band for Vwc2l-1 was detected at 669 bp, Vwc2l-2 at 539 bp and Vwc2l-3 at 398 bp. (B) Quantitative real time PCR analysis of Vwc2l-1 mRNA expression was performed and the expression of Vwc2l-1 during osteoblast differentiation and mineralization was examined. The values are shown as mean + S.D. based on triplicate assays.

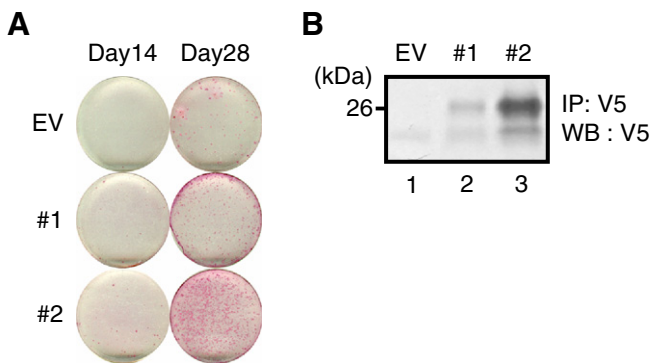


Fig. 3. Effects of Vwc2l overexpression on MC3T3-E1 osteoblast matrix mineralization. (A) Alizarin red staining showed that the extent of mineralized nodule formation was accelerated in both of Vwc2l-1-overexpressing clones (#1 and #2) compared to that of an empty-vector (EV) transfected control clone. (B) The immunoprecipitation (IP)-Western blot (WB) analysis using cultured media derived from EV and Vwc2l clones. The immunopositive bands with anti-V5 antibody were clearly observed and the extent of Vwc2l-V5/His protein expression was correlated with the extent of matrix mineralization in (A). (For interpretation of the references to color in this figure legend, the reader is referred to the web version of this article.)

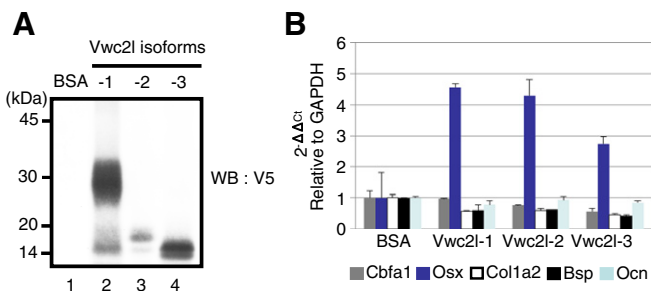


Fig. 4. Effects of Vwc2l isoform proteins on osteoblast differentiation. (A) The immunoreactivity of purified Vwc2l isoform proteins was verified by WB analysis using anti-V5 antibody. Bovine serum albumin (BSA) was used as a negative control. Markers of molecular mass are shown on the left. (B) Quantitative real time PCR analysis of osteogenic marker expression in MC3T3-E1 osteoblastic cells. The values are shown as mean + S.D. based on triplicate assays. Each value represents osteogenic marker expression indicated by color, i.e. Cbfa1 (gray), Osterix/Osx (blue), type I Collagen α 2 chain/Col1a2 (white), bone sialoprotein/Bsp (black), and Osteocalcin/Ocn (light-blue). (For interpretation of the references to color in this figure legend, the reader is referred to the web version of this article.)

Bone sialoprotein and Osteocalcin were quantitatively examined by real time PCR analysis. As shown in Fig. 4B, the expression level of

Osterix, one of the key transcription factors in osteoblasts was clearly increased when any Vwc2l isoform proteins were added (~4.5-fold increase by Vwc2l-1, ~4.2-fold increase by Vwc2l-2 and ~2.8-fold increase by Vwc2l-3). The expression levels of type I collagen α 2 chain and Bone sialoprotein were decreased to some extent by the addition of Vwc2l isoform proteins, whereas those of Cbfa1 and Osteocalcin were essentially same as by BSA addition. These data indicated that Vwc2l isoform proteins increase the certain osteogenic marker expression thereby modulating the matrix mineralization in MC3T3-E1 osteoblast cells and that the common amino acid sequence region to all Vwc2l isoforms is necessary for this modulation.

To date, a number of CKP family members have been cloned and their potential functions in mineralized tissues were characterized [32–35]. Studies in this family proteins may help explore the potential therapeutic means applicable to human skeletal disorders using these proteins' functional domains. Our findings of the identification of novel Vwc2l transcript variants strongly indicate the presence of the functional domain and demonstrate the potential anabolic effect *in vitro*. Interestingly, Vwc2 (also known as Brorin [36]), another member of CKP family is closely related to Vwc2l and we found the presence of Vwc2 protein in bone (our unpublished data), suggesting the critical importance and some redundancy of these two members in bone formation. The expression pattern of Vwc2l in bone and osteoblasts strongly indicate the potential modulatory role of this novel CKP in matrix mineralization. It has been shown that Osterix was initially cloned when induced by BMP-2 addition in myoblastic cells [37], and our data demonstrated that Vwc2l isoform proteins induced Osterix expression in osteoblasts. Although it has been proposed that Brorin-like/Vwc2l antagonizes BMPs [30], it still remains unclear whether Vwc2l antagonizes certain members of BMP family members through its binding. Given the inhibition of BMP-2 induced alkaline phosphatase activity as well as Smad phosphorylation by Brorin-like/Vwc2l was only at moderate level or not observed [30], the effect of Vwc2l on mineralized tissues may be through other specific TGF- β superfamily signaling pathway(s), and the anabolic effect of Vwc2l-derived functional domain on bone formation is currently under investigation.

4. Accession number

The nucleotide sequences for mouse Vwc2-like gene and its transcript variants have been deposited in the GenBank database

under GenBank Accession numbers; EF552208 (Vwc2l-1), EF552209 (Vwc2l-2), EF552210 (Vwc2l-3).

Acknowledgments

This study was supported by grants from the National Institutes of Health (NIAMS-R21AR057451, Y.M.), Boston University, Henry M. Goldman School of Dental Medicine (Y.M.), and Grants-in-Aid for Scientific Research from the Ministry of Education, Culture, Sports, Science, and Technology of Japan (21791928, M.K.).

References

- [1] M.R. Urist, Bone: formation by autoinduction, *Science* 150 (1965) 893–899.
- [2] K. Miyazono, Y. Kamiya, M. Morikawa, Bone morphogenetic protein receptors and signal transduction, *J. Biochem.* 147 (2010) 35–51.
- [3] M. Wan, X. Cao, BMP signaling in skeletal development, *Biochem. Biophys. Res. Commun.* 328 (2005) 651–657.
- [4] N. Kamiya, Y. Mishina, New insights on the roles of BMP signaling in bone: a review of recent mouse genetic studies, *Biofactors* 37 (2011) 75–82.
- [5] S. Chubinskaya, K.E. Kuettner, Regulation of osteogenic proteins by chondrocytes, *Int. J. Biochem. Cell Biol.* 35 (2003) 1323–1340.
- [6] M. Taba Jr., Q. Jin, J.V. Sugai, W.V. Giannobile, Current concepts in periodontal bioengineering, *Orthod. Craniofac. Res.* 8 (2005) 292–302.
- [7] D.W. Walsh, C. Godson, D.P. Brazil, F. Martin, Extracellular BMP-antagonist regulation in development and disease: tied up in knots, *Trends Cell Biol.* 20 (2010) 244–256.
- [8] Y. Nakajima, M. Sakabe, H. Matsui, H. Sakata, N. Yanagawa, T. Yamagishi, Heart development before beating, *Anat. Sci. Int.* 84 (2009) 67–76.
- [9] R.E. Jung, R. Glauser, P. Scharer, C.H. Hammerle, H.F. Sailer, F.E. Weber, Effect of rhBMP-2 on guided bone regeneration in humans, *Clin. Oral Implants Res.* 14 (2003) 556–568.
- [10] R.E. Jung, S.I. Windisch, A.M. Eggenschwiler, D.S. Thoma, F.E. Weber, C.H. Hammerle, A randomized-controlled clinical trial evaluating clinical and radiological outcomes after 3 and 5 years of dental implants placed in bone regenerated by means of GBR techniques with or without the addition of BMP-2, *Clin. Oral Implants Res.* 20 (2009) 660–666.
- [11] D.L. Cochran, A.A. Jones, L.C. Lilly, J.P. Fiorellini, H. Howell, Evaluation of recombinant human bone morphogenetic protein-2 in oral applications including the use of endosseous implants: 3-year results of a pilot study in humans, *J. Periodontol.* 71 (2000) 1241–1257.
- [12] S. Govender, C. Csimma, H.K. Genant, A. Valentin-Opran, Y. Amit, R. Arbel, H. Aro, D. Atar, M. Bishay, M.G. Borner, P. Chiron, P. Choong, J. Cinats, B. Courtenay, R. Feibel, B. Geulette, C. Gravel, N. Haas, M. Raschke, E. Hammacher, D. van der Velde, P. Hardy, M. Holt, C. Josten, R.L. Ketterl, B. Lindeque, G. Lob, H. Mathevon, G. McCoy, D. Marsh, R. Miller, E. Munting, S. Oevre, L. Nordsletten, A. Patel, A. Pohl, W. Rennie, P. Reynders, P.M. Rommens, J. Rondia, W.C. Rossouw, P.J. Daneel, S. Ruff, A. Ruter, S. Santavirta, T.A. Schildhauer, C. Gekle, R. Schnettler, D. Segal, H. Seiler, R.B. Snowdowne, J. Stapert, G. Taglang, R. Verdonk, L. Vogels, A. Weckbach, A. Wentzensen, T. Wisniewski, Recombinant human bone morphogenetic protein-2 for treatment of open tibial fractures: a prospective controlled randomized study of four hundred and fifty patients, *J. Bone Joint Surg. Am.* 84-A (2002) 2123–2134.
- [13] S.D. Boden, T.A. Zdeblick, H.S. Sandhu, S.E. Heim, The use of rhBMP-2 in interbody fusion cages. Definitive evidence of osteoinduction in humans: a preliminary report, *Spine (Phila Pa 1976)* 25 (2000) 376–381.
- [14] M.M. Shah, M.D. Smyth, A.S. Woo, Adverse facial edema associated with off-label use of recombinant human bone morphogenetic protein-2 in cranial reconstruction for craniosynostosis. Case report, *J. Neurosurg. Pediatr.* 1 (2008) 255–257.
- [15] J.D. Smucker, J.M. Rhee, K. Singh, S.T. Yoon, J.G. Heller, Increased swelling complications associated with off-label usage of rhBMP-2 in the anterior cervical spine, *Spine (Phila Pa 1976)* 31 (2006) 2813–2819.
- [16] W. Balemans, W. Van Hul, Extracellular regulation of BMP signaling in vertebrates: a cocktail of modulators, *Dev. Biol.* 250 (2002) 231–250.
- [17] W. Singhatanadgit, V. Salih, I. Olsen, Shedding of a soluble form of BMP receptor-IB controls bone cell responses to BMP, *Bone* 39 (2006) 1008–1017.
- [18] M.C. Fisher, Y. Li, M.R. Seghatoleslami, C.N. Dealy, R.A. Kosher, Heparan sulfate proteoglycans including syndecan-3 modulate BMP activity during limb cartilage differentiation, *Matrix Biol.* 25 (2006) 27–39.
- [19] T. Imamura, M. Takase, A. Nishihara, E. Oeda, J. Hanai, M. Kawabata, K. Miyazono, Smad6 inhibits signalling by the TGF-beta superfamily, *Nature* 389 (1997) 622–626.
- [20] H. Zhu, P. Kavsak, S. Abdollah, J.L. Wrana, G.H. Thomsen, A SMAD ubiquitin ligase targets the BMP pathway, affects embryonic pattern formation, *Nature* 400 (1999) 687–693.
- [21] S.A. Holley, P.D. Jackson, Y. Sasai, B. Lu, E.M. De Robertis, F.M. Hoffmann, E.L. Ferguson, A conserved system for dorsal-ventral patterning in insects and vertebrates involving sog and chordin, *Nature* 376 (1995) 249–253.
- [22] Y. Sasai, B. Lu, H. Steinbeisser, E.M. De Robertis, Regulation of neural induction by the Chd and Bmp-4 antagonistic patterning signals in *Xenopus*, *Nature* 376 (1995) 333–336.
- [23] L.B. Zimmerman, J.M. De Jesus-Escobar, R.M. Harland, The Spemann organizer signal noggin binds and inactivates bone morphogenetic protein 4, *Cell* 86 (1996) 599–606.
- [24] M. Wijgerde, S. Karp, J. McMahon, A.P. McMahon, Noggin antagonism of BMP4 signaling controls development of the axial skeleton in the mouse, *Dev. Biol.* 286 (2005) 149–157.
- [25] Y. Mochida, D. Parisuthiman, M. Kaku, J. Hanai, V.P. Sukhatme, M. Yamauchi, Nephrocyan, a novel member of the small leucine-rich repeat protein family, is an inhibitor of transforming growth factor-beta signaling, *J. Biol. Chem.* 281 (2006) 36044–36051.
- [26] Y. Mochida, M. Kaku, K. Yoshida, M. Katafuchi, P. Atsawasuwan, M. Yamauchi, Podocan-like protein: a novel small leucine-rich repeat matrix protein in bone, *Biochem. Biophys. Res. Commun.* 410 (2011) 333–338.
- [27] Y. Mochida, W.R. Duarte, H. Tanzawa, E.P. Paschalis, M. Yamauchi, Decorin modulates matrix mineralization in vitro, *Biochem. Biophys. Res. Commun.* 305 (2003) 6–9.
- [28] D. Parisuthiman, Y. Mochida, W.R. Duarte, M. Yamauchi, Biglycan modulates osteoblast differentiation and matrix mineralization, *J. Bone Miner. Res.* 20 (2005) 1878–1886.
- [29] S. Pornprasertsuk, W.R. Duarte, Y. Mochida, M. Yamauchi, Overexpression of lysyl hydroxylase-2b leads to defective collagen fibrillogenesis and matrix mineralization, *J. Bone Miner. Res.* 20 (2005) 81–87.
- [30] H. Miwa, A. Miyake, Y. Kouta, A. Shimada, Y. Yamashita, Y. Nakayama, H. Yamauchi, M. Konishi, N. Itoh, A novel neural-specific BMP antagonist, Brorin-like, of the Chordin family, *FEBS Lett.* 583 (2009) 3643–3648.
- [31] Y. Mochida, D. Parisuthiman, S. Pornprasertsuk-Damrongrui, P. Atsawasuwan, M. Sricholpech, A.L. Boskey, M. Yamauchi, Decorin modulates collagen matrix assembly and mineralization, *Matrix Biol.* 28 (2009) 44–52.
- [32] M.E. Brunkow, J.C. Gardner, J. Van Ness, B.W. Paepke, B.R. Kovacevich, S. Prohl, J.E. Skonier, L. Zhao, P.J. Sabo, Y. Fu, R.S. Alisch, L. Gillett, T. Colbert, P. Tacconi, D. Galas, H. Hamersma, P. Beighton, J. Mulligan, Bone dysplasia sclerosteosis results from loss of the SOST gene product, a novel cystine knot-containing protein, *Am. J. Hum. Genet.* 68 (2001) 577–589.
- [33] Y. Kassai, P. Munne, Y. Hotta, E. Penttila, K. Kavanagh, N. Ohbayashi, S. Takada, I. Thesleff, J. Jernvall, N. Itoh, Regulation of mammalian tooth cusp patterning by ectodin, *Science* 309 (2005) 2067–2070.
- [34] N. Nakayama, C.Y. Han, L. Cam, J.I. Lee, J. Pretorius, S. Fisher, R. Rosenfeld, S. Scully, R. Nishinakamura, D. Duray, G. Van, B. Bolon, T. Yokota, K. Zhang, A novel chordin-like BMP inhibitor, CHL2, expressed preferentially in chondrocytes of developing cartilage and osteoarthritic joint cartilage, *Development* 131 (2004) 229–240.
- [35] M.E. Binnerts, X. Wen, K. Cante-Barrett, J. Bright, H.T. Chen, V. Asundi, P. Sattari, T. Tang, B. Boyle, W. Funk, F. Rupp, Human Crossveinless-2 is a novel inhibitor of bone morphogenetic proteins, *Biochem. Biophys. Res. Commun.* 315 (2004) 272–280.
- [36] N. Koike, Y. Kassai, Y. Kouta, H. Miwa, M. Konishi, N. Itoh, Brorin, a novel secreted bone morphogenetic protein antagonist, promotes neurogenesis in mouse neural precursor cells, *J. Biol. Chem.* 282 (2007) 15843–15850.
- [37] K. Nakashima, X. Zhou, G. Kunkel, Z. Zhang, J.M. Deng, R.R. Behringer, B. De Crombrughe, The novel zinc finger-containing transcription factor osterix is required for osteoblast differentiation and bone formation, *Cell* 108 (2002) 17–29.